Engineering Journal issn: 0125-8281

Article

Experimental Investigations and CFD Simulations of the Blade Section Pitch Angle Effect on the Performance of a Horizontal-axis Hydrokinetic Turbine

Edwin L. Chica Arrieta[1,*], Cristian Cardona-Mancilla[2], J. Slayton[1], F. Romero[1], Edwar Torres[1], Sergio Agudelo[1], Juan Arbeláez[2], and Diego Hincapié[2]

1 Departamento de Ingeniería Mecánica, Facultad de Ingeniería, Universidad de Antioquia (UdeA), Calle 70 No. 52-21, Medellín, Colombia
2 Instituto Tecnológico Metropolitano (ITM), Calle 73 No. 76-354, Medellín, Colombia
*E-mail: edwin.chica@udea.edu.co (Corresponding author)

Abstract. Three twisted blades of a 1 kW prototype hydrokinetic turbine were designed based on the Blade Element Momentum (BEM) theory with a tip speed ratio of 6.25; a water velocity of 1.5 m/s; an angle of attack and pitch angle of 5 and 0°, respectively; a power coefficient of 0.4382 and a drive train efficiency of 70%. S822 hydrofoil was used to generate the coordinates of the blade cross-section. Experimental investigations and Computational Fluid Dynamics (CFD) simulations were carried out to estimate the performance of the blade design and know the effect of the section pitch angle on the performance of a horizontal-axis hydrokinetic turbine. The obtained results showed that the increase in the section pitch angle enhanced the performance up to a certain value. Further increase in the section pitch angle resulted in a low performance and a reduction of the rotation velocity, which in turn requires a high gearing ratio of the transmission system.

Keywords: Hydrokinetic turbine, blade, section pitch angle, performance.

ENGINEERING JOURNAL Volume 22 Issue 5
Received 15 November 2017
Accepted 6 June 2018
Published 30 September 2018
Online at http://www.engj.org/
DOI:10.4186/ej.2018.22.5.141

DOI:10.4186/ej.2018.22.5.141

1. Introduction

Hydrokinetic turbine blades are shaped to generate the maximum power from water at the minimum cost. Primarily, the design is driven by the hydrodynamic requirements; nevertheless, reasonable construction costs must be considered when shaping the blade. In particular, the blade tends to be thicker than the profile hydrodynamic optimum close to the root, where the stresses due to bending moments are the greatest [1–4].

In general, the optimal design of a horizontal-axis hydrokinetic turbine has been rendered complicated by many parameters, such as the blade profile, blade taper, tip loss, variable water speed, rotation speed, power coefficient, section pitch angle, blade number and the angle of attack, to name just a few. From the engineering design point of view, the more torque (T) has the turbine rotor, the more power (P) will develop the turbine. Thus, it is important to take advance of the maximum possible torque and turbine rotor velocity. Torque and angular velocity of the rotor are achieved by hydrofoil lift and drag forces. These forces depend on the change of pressures generated in the hydrofoil surfaces, which in turn depend on the fluid density and the hydrofoil shape profile, angle of attack and section pitch angle [2, 5–8].

The section pitch angle is the angle between the chord of the blade and the plane of rotation, and is measured at a specific point along the length of the blade. The section pitch angle is equal to the pitch angle along the blade in an untwisted blade, and varies locally in twisted blades. In twisted blades the section pitch angle decreases from the blade root to the tip. On the other hand, the angle of attack of a blade is the angle between the water current and the chord line of the blade profile. The angle of attack for each blade changes at a rate relative to the tip speed of the turbine. When determining the angle of attack needed to obtain the lift coefficient, the right choice is to maximize the lift to drag ratio. Obtaining as much lift as possible and as little drag as possible is preferred, since lift force is converted into usable power and drag force creates losses and reduces the efficiency of the machine [1, 3, 5, 9, 10].

Various studies have been presented in wind domain, which include the relation of the pitch and the performance of the horizontal-axis turbine. However, the performance of a hydrokinetic turbine has been poorly investigated. Some studies show that the adjustment of the pitch angle may control the output power of the turbine when wind velocity changes [11–13]. Due to differences on the use of horizontal-axis turbines in various types of fluids, studies on hydrokinetic turbines still need to be deeply explored for knowing the parameters having a great impact on the turbine performance [14–16].

As it is widely known, the maximization of the power is fundamental in the hydrokinetic turbine design in order to improve the extraction of energy from water flow; therefore, the objective of this paper is to investigate experimentally and numerically the effect of the section pitch angle on the performance of a hydrokinetic turbine of 1 kW designed for a water velocity (V) of 1.5 m/s with a tip speed ratio (λ) of 6.325; an initial angle of attack (α) and pitch angle (θ) of 5° and 0°, respectively; a power coefficient (C_p) of 0.4382; a drive train efficiency (η) of 70 % and a S822 hydrofoil profile. The turbine consists of a rotor with three blades of radius (R) equal to 0.79 m. The experimental investigations on the performance of a scale-model three-blades operating under different water velocities were conducted in a recirculating water channel.

2. Numerical Method

In the optimization design of the rotor, maximizing the power percentage to be extracted from the water current and providing enough strength to the blade structure are of special importance. Consequently, a detailed hydrodynamic analysis of the rotating hydrofoil must be carried out. In general, hydrofoil must be designed starting from the premise that fluid mechanic parameters, such as the angle of attack and the homogeneous pressure distribution, must be maintained along the whole wingspan, despite the fact that rotary operating conditions produce different linear velocities of rotation along the blade axis, which are higher as the point is nearer from the blade tip. The design method of the main characteristics of the hydrokinetic turbine rotor is based on simplifying assumptions and theoretical design optimum

principles previously defined and verified in practice for wind turbine [2, 5, 17–19].

Generally, the performance of the rotor can be determined by various geometric and flow parameters; i.e., for a fixed diameter of the rotor there are various factors influencing energy production: the rotor rotation velocity, flow velocity, power coefficient, blade number, tip speed ratio, blade shape, section pitch angle, angle of attack, hydrofoil chord distribution, etc. Perhaps, among these factors, the most important is the blade hydrofoil shape, which should be selected on the basis of high efficiency; i.e., high lift and low drag [6, 7, 19]. The hydrofoil shape, the mass distribution and the location of the shaft determine the inertial moment of the blade that affects the efficiency of the turbine. For example, for a fixed rotational velocity, the increase of the inertial moment of the blade can result in an increases kinetic energy of the rotor, as well as its efficiency. Nevertheless, the effect of the moment of inertia on the efficiency of the turbine was neglected in this study.

In this regard, the effect of the section pitch angle (γ) on the hydrokinetic turbine performance was numerically investigated by solving the steady 3D incompressible Reynolds Averaged Navier-Stoke equations. Therefore, a finite volume based on the ANSYS CFX solver was used to solve the hydrodynamic equations. As observed in Fig. 1, the section pitch angle (γ) is equal to the sum of pitch angle (θ) and the twist angle (β), and represents the mechanical angle between the hydrofoil chord and its plane of rotation. On the other hand, the angle of attack, which is represented by α, is the geometric angle between the relative velocity vector (V_{Rel}) and the chord line (Fig. 1). This angle depends on the hydrofoil profile and its section pitch angle.

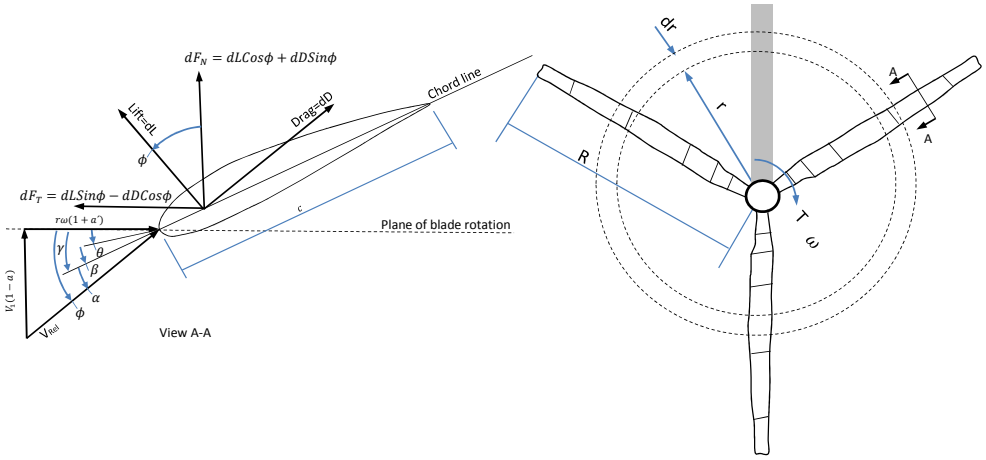

Fig. 1. Blade element model of the axial hydrokinetic turbine.

Despite the rotating condition, maintaining the angle of attack along the wingspan ir required. This scenario allows keeping the rotor fluid dynamic stability. These commitments are accomplished by varying the geometric parameters of the hydrofoil chord (l), the section pitch angle (γ) and the twist angle (β) along the wingspan. To achieve this goal the Blade Element Theory was used. Figure 2(a) provides the specifications of the designed hydrokinetic turbine. The turbine rotor diameter was 1.58 m, and it had three blades. It should be noticed that turbines with 3 blades are more stable and do not cause much vibration, increasing the bearing life and reducing fatigue failures. Additionally, 3-bladed turbines have lower TSR than 2-bladed ones, which reduces the chance of cavitation inception [16, 20]. In the current work, each blade was 0.79 m long. The blades were developed with the profile shape of a S822 and with a chord, thickness and twist distribution presented in Fig. 2(b). The water velocity considered for the design was 1.5 m/s. After finding the value of c and the twist angle for every section, the next step was to multiply the values of the chord by the non-dimensional coordinates of the S822 profile. The values of x and y coordinates of the profile for each section were exported to parametric 3D design software. Therefore, the cross sections of the blade were created at different distances from the root to the tip, and, using the Loft command, a 3D model of the whole blade was produced [21, 22]. The resulting image is shown in Fig. 2. During the process, the first section near the blade root was

DOI:10.4186/ej.2018.22.5.141

removed and the second section of the blade profile was modeled with the same twist angle of the third section. Furthermore, in order to improve the structural strength of the blade, a corrective factor (Fc) was introduced. Fc was equal to 3.8. Thus, the values of each chord length calculated were multiplied by this factor.

Power	1 kW
Hydrofoil	S822
Density	997 kg/m^3
Rotor radius	0.79 m
Number of blades	3
Blade pitch	0°
Rotor speed	12.009 rad/s
Fluid speed	1.5 m/s

a

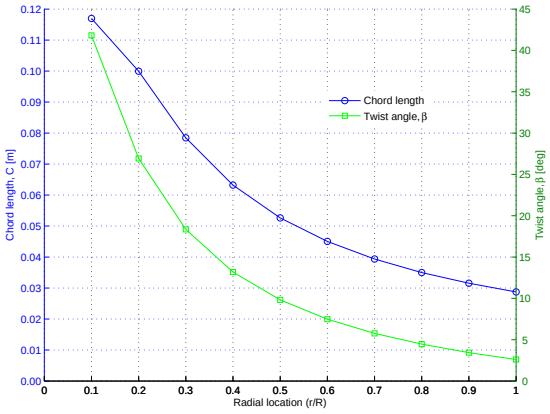

b

Fig. 2. (a) Specifications of the turbine used for simulation studies, and (b) Chord and twist distribution.

2.1. Governing Equations

A three-dimensional CFD analysis was performed in ANSYS CFX using a multiple reference frames technique in order to study the performance of the hydrokinetic turbine computationally. It is widely known that for all fluid flow problems, the mathematical model is based on the fundamendal mass, momentum and energy conservation equations. In the case of a hydrokinetic turbine, numerical modelling is complicated due to the rotation of the turbine blades coupled with turbulence and stall effects. A moving reference frame was, therefore, incorporated to take the blade rotation into account and transform the unsteady flow in an inertial (stationary) frame to a steady flow in the non-inertial (moving) frame. When a moving reference frame is activated, the equations of motions are modified to incorporate the additional acceleration terms which occur due to the transformation from the stationary to the moving reference frame [23–25]. Solving these equations in a steady state manner, the flow around the moving parts can be modeled. When the equations of motion are solved in the rotating reference frame, the equation are computed using relative velocity formulation. For the relative velocity formulation, the equation for conservation of mass or continuity can be written as Eq. (1).

$$\nabla.\overrightarrow{U_r} = 0 \tag{1}$$

On the other hand, the conservation equation for momentum can be expressed as Eq. (2).

$$\rho\left[\frac{\partial\overrightarrow{U_r}}{\partial t} + \nabla.\left(\overrightarrow{U_r}\overrightarrow{U_r}\right) + \left(2\overrightarrow{\Omega}x\overrightarrow{U_r} + \overrightarrow{\Omega}x\overrightarrow{\Omega}x\overrightarrow{r}\right)\right] = -\nabla p + \nabla.\tau_r \tag{2}$$

where ρ, is the water density (997 kg/m^3) $\overrightarrow{U_r}$ is the relative velocity viewed from rotating reference frame, Ω is the rotational speed of the turbine, $\left(2\overrightarrow{\Omega}x\overrightarrow{U_r}\right)$ is the Coriolis force, $\rho\left(\overrightarrow{\Omega}x\overrightarrow{\Omega}x\overrightarrow{r}\right)$ is the centrifugal force and ∇p is the pressure gradiend across the turbine. The viscous tensor (τ_r) is defined as Eq. (3).

$$\tau_r = \mu_{eff}\left[\left(\nabla\overrightarrow{U} + \nabla\overrightarrow{U}^T\right) - \frac{2}{3}\nabla.\overrightarrow{U}I\right] \tag{3}$$

where U is the absolute fluid velocity and I is the identity tensor. The molecular viscosity (μ_{eff}) is the sum of the dynamic viscosity (μ) and turbulent viscosity (μ_t); being calculated from a representative turbulence model. Among different turbulence models existing in the literature, the $k-\omega$ shear stress transport (SST) model was chosen for the analysis due to its capability of providing accurate flow-field predictions under adverse pressure gradient and separated flow conditions, both, conditions considered as prevalent in hydrokinetic turbine performance [23, 26–29].

2.2. Computational Domain

Based on the characteristics of the cyclic symmetry for the structure of the hydrokinetic turbine rotor (Fig. 2), a rotor sector conformed of a blade and a hub angle of 120° was used to run the CFD simulation. The computational domain was divided into two parts: an inner rotatable part, with high density of elements, and an outer stationary part with low density elements [30]. Accordingly, a rotational periodic boundary condition was applied across the back and bottom surfaces of the computational domain shown in Fig. 3. The computational domain was created using Nx and meshed in ANSYS ICEM CFD. The mesh used was an unstructured (primarily hexahedral) mesh with very fine prims layer near the turbine walls. All dimensions of the boundary were given in terms of radius (R) of the turbine. The turbine possesses 120° periodicity and, hence, only one blade was modeled. Figure 3 shows the location of the turbine within the computational domain. The turbine rotational plane was located R away from the inlet, and the fluid domain was extended 7R behind the turbine rotational plane to capture the near and far wake effects. Through previous numerical simulations, it was check that the domain length (7R) was adequate to guarantee that the flow is fully developed downstream of the turbine. The radius of the blade was always fixed during the study, only the section pitch angle of the blade (γ) was varied between 0° and 90° to determine the relationships between turbine geometrical design and performance.

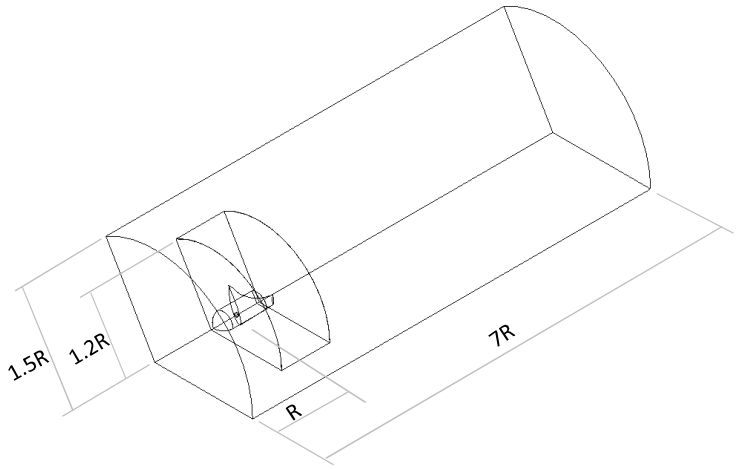

Fig. 3. Computational domain used for CFD analysis.

The mesh was imported into CFX and, then, the boundary conditions were applied to the computational domain. The study assumed steady and incompressible flow. The velocity inlet boundary condition was applied on the left surface of the domain with uniform axial (free-stream) velocity of 1.5 m/s. A pressure outlet boundary condition was provided on the right surface with zero gauge pressure (this boundary condition was applied because the length of the computational domain guarantees that the flow is fully developed downstream of the turbine), and gravity was included in the model.

Additionally, realizable $k-\omega$ turbulence model was chosen. The turbulence intensity of 5% was defined. The no-slip condition was applied to the turbine blade and hub walls; i.e., the relative velocity of the surface blade and hub was set at zero. The internal surfaces defining the cylindrical rotary connection between the subdomain that contains the rotor and the stationary field were linked using the condition of frozen rotor. Thus, the components of the fixed domain were transformed into a moving

reference system, adding the Coriolis and centrifugal acceleration, enabling local flow characteristics to be transported through the interface.

A good quality CFD model design requires mesh refinement to achieve a grid-independent solution. Therefore, a mesh independent test was conducted by increasing the number of elements of the mesh until the torque of the turbine did not experience hardly any variation by refining the mesh. Thus, an unstructured tetrahedral mesh was used. The final mesh consisted of 9.529.801 nodes.

2.3. Numerical Results

It is important to note that the hydrokinetic turbine performance is characterized by its power coefficient (C_P) that represents the relationship between the power extracted from water current and the power available in the current flowing through the same area as projected by the turbine. This coefficient can be calculated by Eq. (4).

$$C_P = \frac{P}{0.5\rho\pi R^2 V^3} \tag{4}$$

$$P = T\omega \tag{5}$$

where P is the power output obtained from Eq. (5), T is the torque on the turbine shaft, ρ is the water density, V is the water current velocity, R is the rotor radius and ω is the angular velocity of the rotor. The maximum achievable power coefficient is 59.26%, and it is designated as the Bezt limit. In practice, values of obtainable power coefficients are in the range of 45%. Values below the theoretical limit are caused by the inefficiencies and losses attributed to different configurations, rotor blade and turbine designs. The angular velocity is usually represented as a tip speed ratio (λ), which is a relationship between the turbine blade velocity and the current velocity. There is a λ point where the hydokinetic turbine can perform the maximum energy extraction. λ can be defined as Eq. (6):

$$\lambda = \frac{R\omega}{V} \tag{6}$$

The simulation allowed computing the torque (T) on the blades for various section pitch angles and angular velocities (ω), which was subsequently multiplied by the blade total number (3) and the angular velocity. Thus, the maximum turbine power output was calculated (1063.5 W), for a section pitch angle of 5°. This value was compared to the design power (1000 W). The good agreement between the numerical and theoretical turbine power output enabled to validate the design of the rotor. The predicted normalized rotor power values at various blade section pitch angles for a water speed 1.5 m/s are shown in Fig. 4(a). The normalized power represents the ratio between the power output for a specific pitch angle of the blade section and the maximum power obtained when the section pitch angle is equal to 5°. It is clearly observed from Fig. 4(a) that this angle affects the turbine power output.

On the other hand, the relationship between the power coefficient C_p and the tip speed ratio is shown in Fig. 4(b) for different section pitch angles. It can be noticed that a maximum is reached at different positions for different section picth angles. For section pitch angles of 5° and 10°, minimal changes in C_p were found for values of λ between 0 and around 6. The maximum efficiencies of the hydrokinetic turbine reach levels above 44.9% but below the Betz limit when the section pitch angle and λ are equal to 5 ° and 11.03 respectively. In this regard, the optimum blade angle for this turbine was determined to be 5°; thus, the highest power occurred at this angle.

In general, it is possible to appreciate from the simulation results that when the fluid moves over the hydrofoil, the velocity of the fluid particles at the upper surface becomes higher than that of the lower surface, due to the section pitch angle and the angle of attack. A high velocity generates a low pressure zone at the upper surface of the hydrofoil, while low velocity at the lower surface produces a high pressure zone. Unequal pressure distribution between two surfaces of the hydrofoil creates the lift force. The direction of the lift force is normal to the chord line. The torque and angular velocities are achieved by the hydrofoil lift forces. As the lift in the blades is increased, more torque and angular

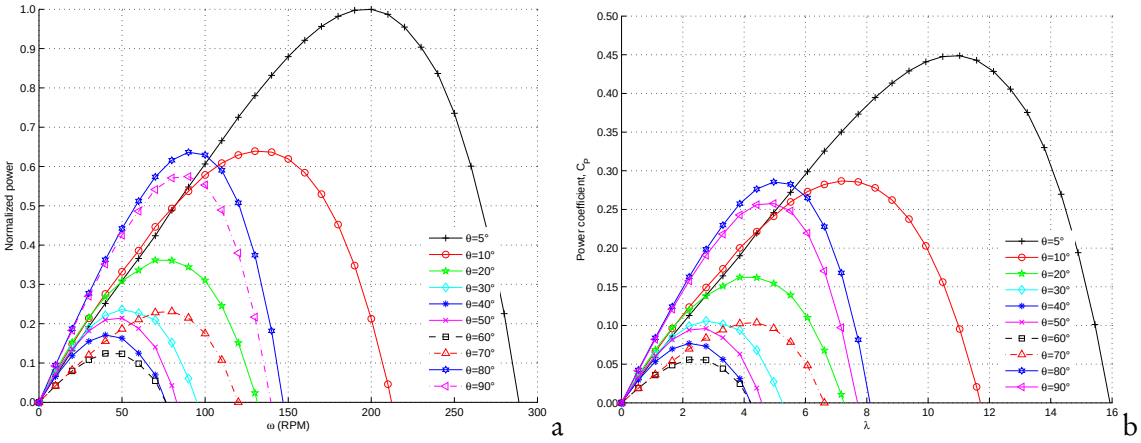

Fig. 4. (a) Computed rotor power at various section pitch angles and angular velocities; (b) Power coefficient as a funtion of the tip speed ratio (λ) for differents section pitch angles.

velocity can be obtained. If the section pitch angle is increased, the torque could increase up to a certain angle since the lift forces could increase. After this angle, the torque could decrease.

Furthermore, the results indicate that at a low rotation, the turbine with high section pitch angle performs better than those with lower angle. This condition is reserving at the high rotation. Similar results were obtained by Coiro et al. in 2015, Batten et al. in 2006 and Balaka & Rachaman in 2012 [4, 14, 31].

To examine the influence of the blade section pitch angle on performing the hydrokinetic turbine, an experimental set-up was constructed. Similarities between the CFD model and the experimental set-up were carefully considered. In general, the experimental behavior of the turbine was very similar to the behavior described from the numerical results detailed previously. Therefore, by increasing the section pitch angle above 10° a reduction in the power and power coefficient of hydrokinetic turbine in both models: numerical and experimental is caused.

3. Experimental Setup

Experiments were used to predict the optimal section pitch angle that produces maximum power outputs of the horizontal-axis hydrokinetic turbine. The experiments were performed in a recirculating water channel at the Universidad de Antioquia, in Colombia. Flow velocity measurements in the channel were obtained using a PCM Pro flow meter with an accuracy of $\pm$ 1% and $\pm$ 2% of the measured value for velocity and flow, respectively. A hydrokinetic turbine model with a diameter (D) of 0.24 m was subjected to a uniform steady flow and its performance was evaluated for different blade pitch angles via power measurements.

3.1. Recirculating Water Channel

The experiments were conducted in a recirculating water channel with rectangular cross section of 310x500 mm and 8 m of length, shown schematically in Fig. 5. It was powered by a 14.9 kW electric motor driving an axial flow impeller and producing flow velocities up to 1 m/s. The channel included large span acrylic sections that provide complete visual access from the sides as well as from the bottom. The feed plenum and internal components were designed to guarantee fully developed flow within 2.5 m of the channel entrance. The exhaust plenum provided the fluid flow level adjustment through the use of a weir assembly.

DOI:10.4186/ej.2018.22.5.141

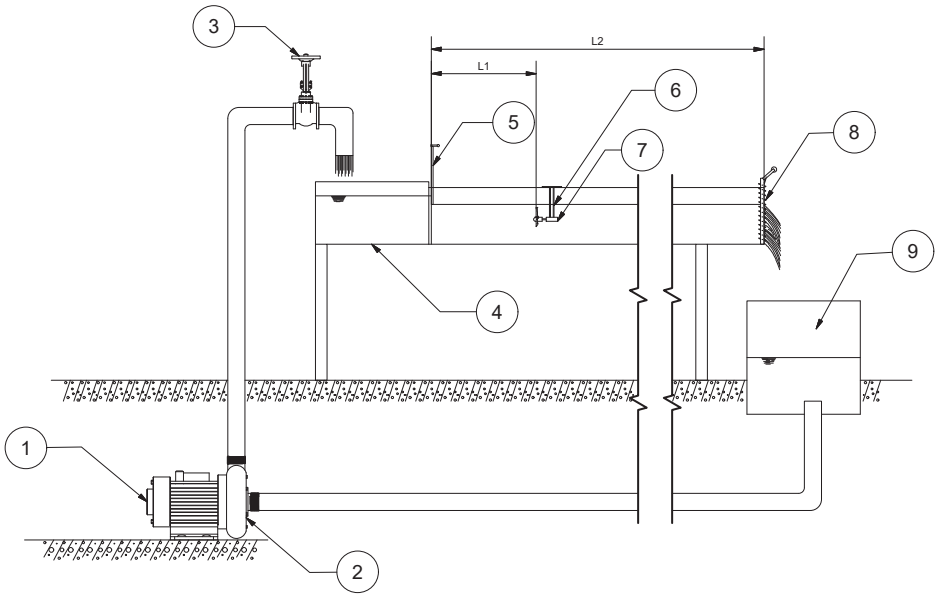

Fig. 5. Schema of the recirculating water channel. Working section (length, L2= 8 m, width = 0.31 m, depth = 0.5 m). 1) Motor of 14.9 kW, 2) Impeller, 3) Water inlet valve, 4) Channel, 5) Gate, 6) Model horizontal-axial hydrokinetic turbine, 7) Rotary torque sensor, 8) Weir assembly, 9) Feed tank.

3.2. Horizontal-axis Hydrokinetic Turbine Scale Model

The turbine used during the experiments had a horizontal axis and, for this study, it was fitted with three blades. It had a diameter of 0.24 m. The blade profile employed was S822 and they were manufactured accurately and economically with the use of a CNC machining center. In order to be able to manufacture each blade, a number of conditions must be taken into account. First of all, the geometry of the part and the appropriate tools for the machining of the surface must be selected so that the tools cutting surface are able to manufacture and remove material from the specific geometric places. Secondly, the tools must be constantly in contact with the surface, so as to manufacture it smoothly and accurately. Thirdly, the radius of the tool surface must be calculated so that the curves of the blade surface are correctly manufactured. Finally, the forth condition is the position of the cutting tool at the surface in order to appropriately manufacture the stock and prevent from any fault positioning.

For the blade manufacturing, the CAD file was imported into CAM software Nx for further analysis. With the aid of this software, the strategy of the blades manufacturing was decided and programmed with respect to the quality of the final product, addressed through a parameter of great importance, namely surface roughness and the required machining time. The manufacturing process took place in a CNC machining center Milltronics VM20 with four axes indexed. The tools used were a flat end mill of diameter equal to 25.4 mm and two ball end mills tool with 12 mm and 8 mm of diameter. The workpiece material employed was aluminum AA7075-T6 (shown in Fig. 6). In general, the complex geometry of the blade, although it is a challenge for the machining process, modern software and cutting and machine tools can overcome any problem imposed and realize the final workpiece geometry in relatively low machining times and with high quality characteristics.

Once the blades and the hub were made (shown in Fig. 7), the turbine was connected to a waterproof housing, containing a rotary torque sensor with encoder (Futek-Model TRS605 with an accuracy of $\pm$0.000153), which measures the rotor angular velocity and torque. The angular velocity and torque were used to calculate the power output (P). The capacity of the torque sensor was 20 Nm. The TRS605 utilizes metal foil strain gauge technology and features non-contact signal transmission allowing the sensor to operate at up to 7000 RPM.

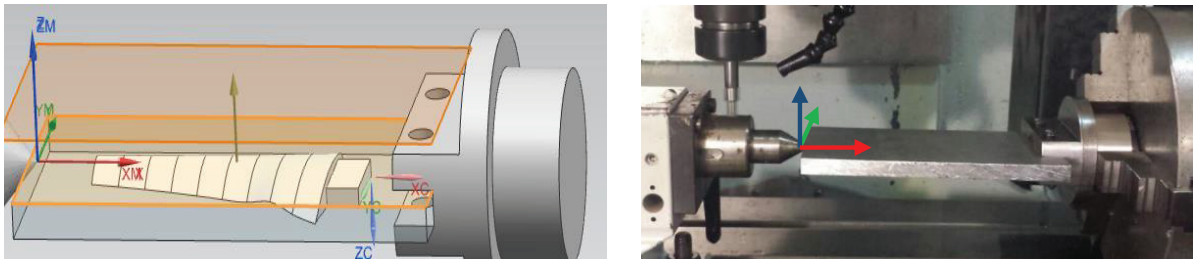

Fig. 6. CAM software snapshots and real machining process.

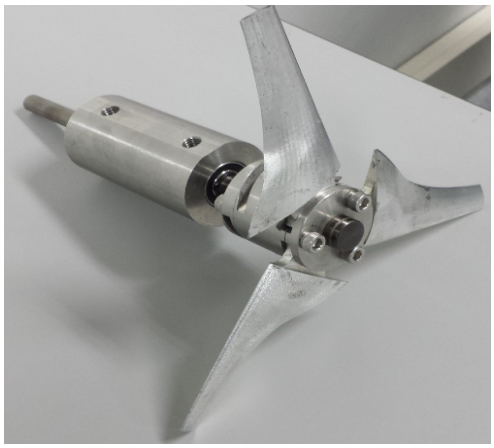

Fig. 7. Scale model of the hydrokinetic turbine.

3.3. Methodology

The turbine was installed at a distance of $L_1 = 3$ m of the channel entrance and a deep of 0.5 m, where the flow was fully developed. This position of the turbine was kept during the whole experimental tests. The inlet velocity of the flow was varied during the test and obtained using a PCM Pro flow meter. It was measured in three different positions in the channel upstream of the turbine and averaged to determine the flow velocity. This work was focused on the effects of the blade section pitch angle on the performance of a horizontal-axis hydrokinetic turbine. Therefore, during the experiment, the blade section pitch angle was changed (Fig. 8). Measurements were taken at different blades pitch angles with several current conditions. The three blades of the turnine were always set at the same blade pitch angle and for the experiments, six different section pitch angles were tested (-15°, 0°, 10°, 18° ,20°, 25°).

Turbine power was calculated by measuring the torque and the angular velocity at the output of the shaft using a rotary torque sensor with encoder (Futek-Model TRS605). The sensor was fully coupled to the turbine shaft and a drive brake (Fig. 9) for measuring the torque and the angular velocity and, subsequently, the power developed by the turbine when the rotor was loaded. Data were collected in real time using intelligent digital hand held display (IHH500 Pro) connected to the sensor. For each test run the velocity of the current was kept as uniform as possible and the data acquisition equipment was switched on. Additionally during each experiment, the turbine was loaded by the electromagnetic brake and the rotating velocity and torque were measured in each load.

With the values of water speed, rotor rotating speed and the rotor torque measured by the sensor, the power coefficient and power outputs from the turbine were calculated using Eq. (4) and (5), respectively.

DOI:10.4186/ej.2018.22.5.141

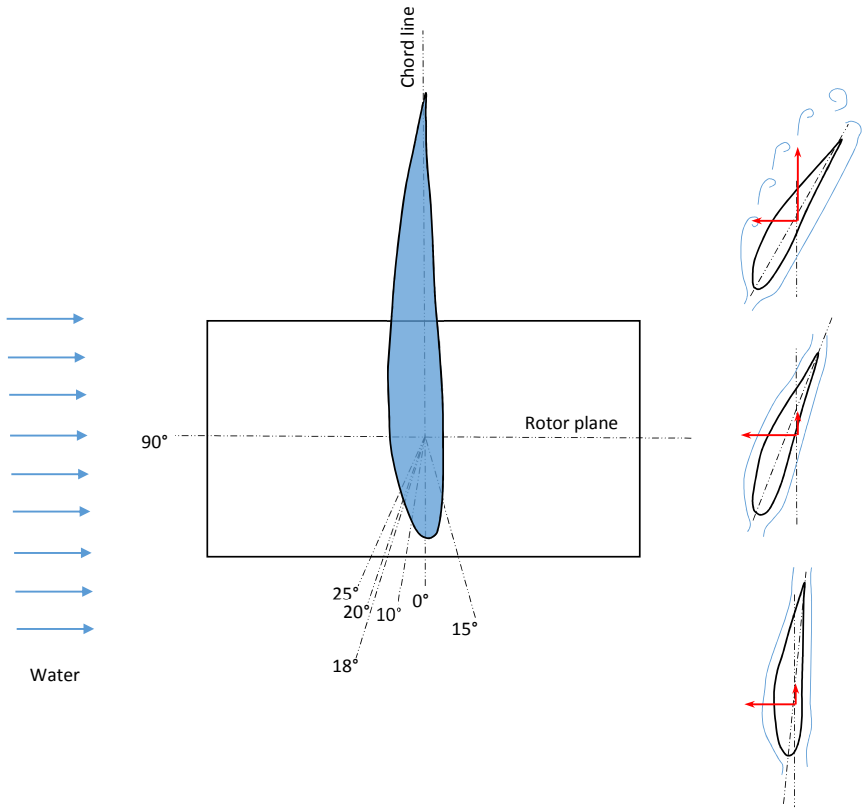

Fig. 8. Section pitch angle variation details.

3.4. Experimental Results and Discussions

From the experimental results, it can be concluded qualitatively that at very low section pitch angles, the water flow over the hydrofoil is essentially smooth and laminar with a slight small amount of turbulence occurring at the trailing edge of the hydrofoil (Fig. 8). The point at which laminar flow ceases and turbulence begins is known as the separation point. By increasing the section pitch angle, the area of the hydrofoil facing directly into water. This results in a rise of the lift; however, it also moves the separation point of the laminar flow of the water above the hydrofoil part way up towards the leading edge and the result of the increased turbulent flow above the hydrofoil is an increase in the drag. Maximum lift typically occurs when the section pitch angle is around 10°. Above 10°, the separation point moves right up to the leading edge of the hydrofoil a laminar flow above the hydrofoil is destroyed. The increase of turbulence can cause the rapid deterioration of the lift force while at the same time it dramatically increases the drag and should result in a stall of the rotor.

On the other hands the power coefficient against the tip speed ratio for different pitch angles was analyzed. The effect of the pitch angle is shown in Fig. 10. From the figure, the horizontal axis shows the tip speed ratio (λ) and the vertical axis, the power coefficient (C_p).

It can be concluded that the performance increases at a low section pitch angle (below 10°). It indicates that for values below 10°, the turbine converts kinetic energy of the current into mechanical energy more efficiently than for other values. In this experiment, the highest values of power coefficient were 0.443, 0.424, and 0.442 for 10°, 0° and -15°, respectively. For blade section pitch angle values greater than 10°, obtaining high performances is very difficult, due to the rotation velocity is reduced, which in turn requires a high gearing ratio of the transmission system with the subsequent increase in the cost of the turbine. Moreover, the measures of the turbine power outputs at different section pitch angles are shown in Fig. 11. The values of the theoretical available power are calculated using Eq. (4). these values depend on the radius of the rotor ($R = 0.12m$), the water density ($\rho = 997kg/m^3$), the power coefficient (0.4382) and the water velocity; which are resented in Fig. 11.

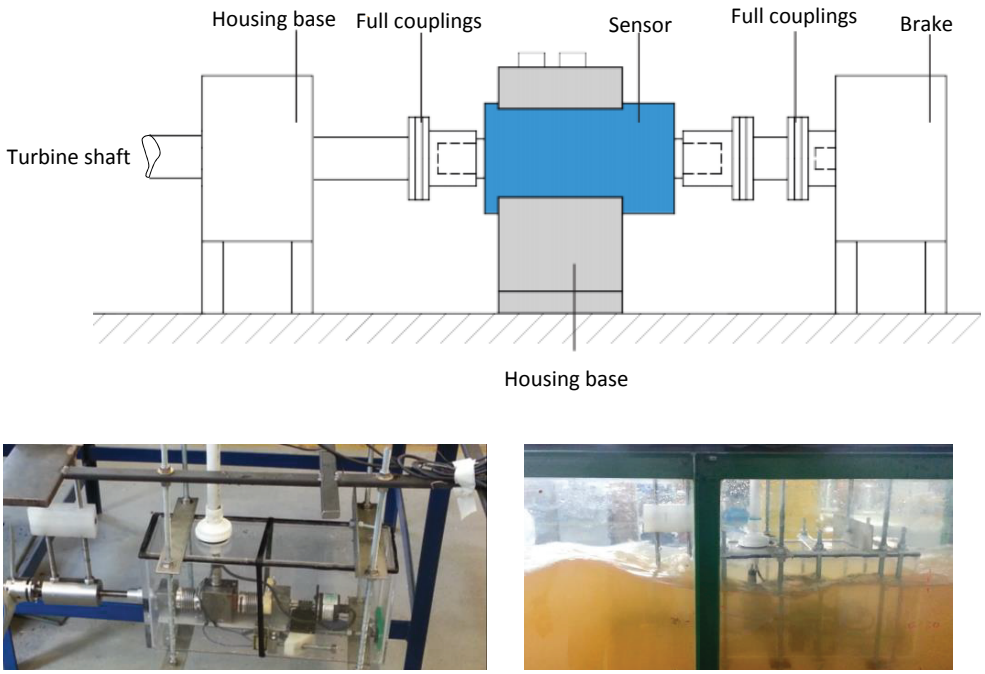

Fig. 9. Installation of the torque sensor.

Figure 11 clearly shows that with the increase in water velocity, the power output of the turbine increases at a much higher rate for blade section pitch angles between -15 and 10°, while it increases at a much lower rate for 25°. The study shows that a negative pitch angle also provides a good performance of the turbine. It is also very clear from Fig. 11 that an increase in the blade section pitch angle causes greater reductions in the magnitude of the power output from the turbine for values greater than 10°.

The blade pitch angle is very promising for the performance optimization of hydrokinetic turbine since it is very simple to apply in practice and does not introduce high manufacturing, installation or maintanance costs. The numerical results are closely comparable with experimental results. The studies show that increasing the pitch angle enhances the turbine performance up to a certain value. Further increase in the pitch angle above 10° may result in the turbine performance decrease.

4. Conclusion

The maximization of the power coefficient is fundamental in the hydrokinetic turbine design in order to improve the extraction of energy from water flow in rivers currents. Therefore, the influence of the pitch angle on the hydrodynamic performance of the horizontal-axis hydrokinetic turbine was investigated both experimentally and numerically. The blade profile employed was S822. The experiments were carried out in a recirculating water channel. From the experimental results the highest value of C_P was observed at a pitch angle of 10° and numerical results showed that high performance can be obtained by the turbine with blade section pitch angles of 5° at high rotation operations. Additionally, the numerical results show that for section pitch angles between 5° and 10°, minimal change in C_p were found for values of λ between 0 and around 6. The differences were always less than 5% of the power coefficient.

CFD was also used to simulate the three-dimensional unsteady flow and turbulence characteristics around the turbine blade. For that purpose, the commercial software ANSYs was used. The results verified the experimental findings.

In summary, the experimental and numerical investigation presented in this work paper contributes to the characterization of the the hydrokinetic turbine hydrodynamic performance and to a better understanding on the physical phenomenon involved around the turbine performance.

DOI:10.4186/ej.2018.22.5.141

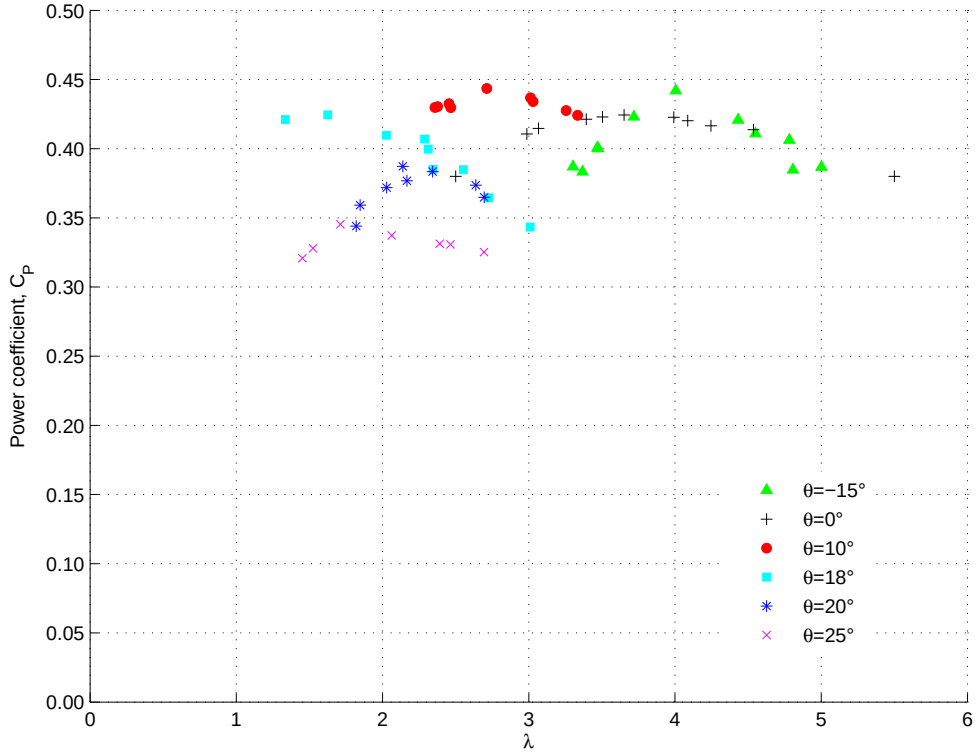

Fig. 10. Effects of the blade section pitch angles on the rotor performance.

Acknowledgments

The authors gratefully acknowledge the financial support from the Colombian Institute of Science and Technology (COLCIENCIAS) and the Universidad de Antioquia.

References

[1] A. Muratoglu and M. I. Yuce, "Performance analysis of hydrokinectic turbine blade sections," *Advances in Renewable Energy*, vol. 5, pp. 1–10, 2015.

[2] M. Anyi and B. Kirke, "Evaluation of small axial ow hydrokinetic turbines for remote communities," *Energy for Sustainable Development*, vol. 14, no. 2, pp. 110–116, 2010.

[3] E. Rosenberg, A. Lind, and K. A. Espegren, "The impact of future energy demand on renewable energy production case of norway," *Energy*, vol. 61, pp. 419–431, 2013.

[4] W. M. J. Batten, A. S. Bahaj, A. F. Molland, and J. R. Chaplin, "Hydrodynamics of marine current turbine," *Renewable Energy*, vol. 31, no. 2, pp. 249–256, 2006.

[5] A. Muñoz, L. Chiang, and E. D. la Jara, "A design tool and fabrication guidelines for small low cost horizontal axis hydrokinetic turbines," *Energy for Sustainable Development*, vol. 22, no. Supplement C, pp. 21 – 33, 2014, wind Power Special Issue.

[6] H. J. Vermaak, K. K., and K. S. P., "Status of micro-hydrokinetic river technology in rural applications: A review of literature," *Renewable and Sustainable Energy Reviews*, vol. 29, pp. 625–633, 2014.

[7] M. S. Gney and K. Kaygusuz, "Hydrokinetic energy conversion systems: A technology status review," *Renewable and Sustainable Energy Reviews*, vol. 14, no. 9, pp. 2996–3004, 2010.

[8] M. J. Khan, G. Bhuyan, I. M. T., and Q. J. E., "Hydrokinetic energy conversion systems and assessment of horizontal and vertical axis turbines for river and tidal applications: A technology status review," *Applied Energy*, vol. 86, no. 10, pp. 1823–1835, 2009.

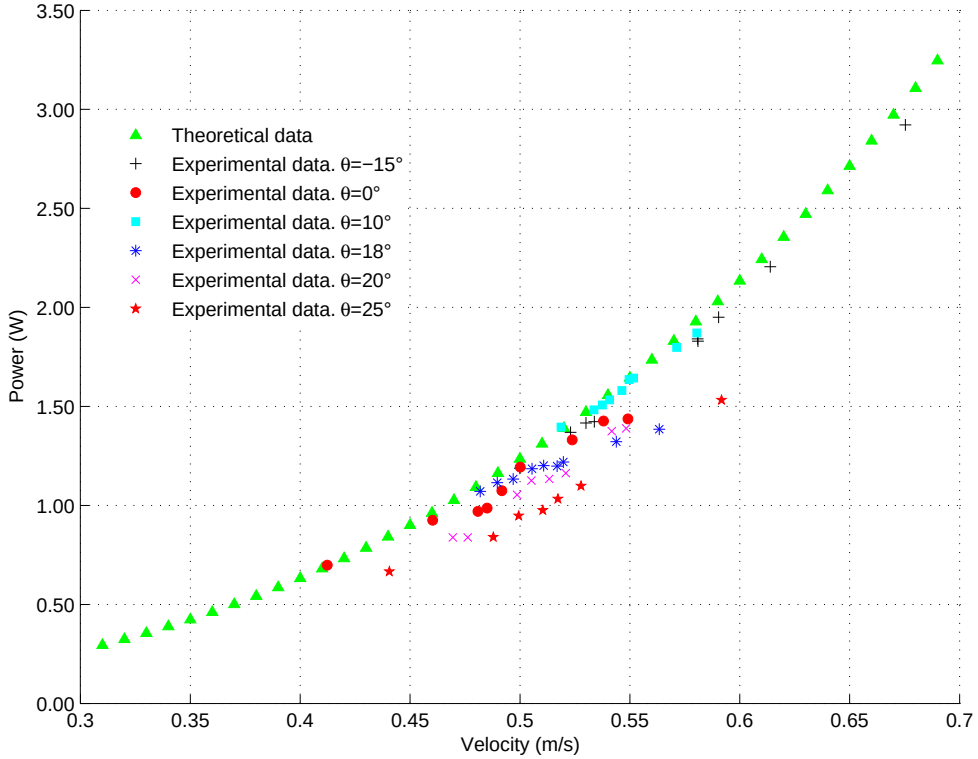

Fig. 11. Experimental and theoretical results of the power output from the hydrokinetic turbine.

[9] R. H. van Els and A. C. P. Brasil, Jr., "The brazilian experience with hydrokinetic turbines," *Energy Procedia*, vol. 75, no. Supplement C, pp. 259 – 264, 2015, clean, Efficient and Affordable Energy for a Sustainable Future: The 7th International Conference on Applied Energy (ICAE2015).

[10] L. I. Lago, F. L. Ponta, and L. Chen, "Advances and trends in hydrokinetic turbine systems," *Energy for Sustainable Development*, vol. 14, no. 4, pp. 287 – 296, 2010.

[11] M. G. Khalfallah and A. M. Koliub, "Suggestions for improving wind turbines power curves," *Desalination*, vol. 209, no. 1, pp. 221–229, 2007.

[12] J. F. Manwell, J. G. McGowan, and A. L. Rogers, *Wind Energy Explained: Theory, Design and Application*. Wiley, 2009, pp. 23–155.

[13] G. Riegler, "Principles of energy extraction from a free stream by means of wind turbines," *Wind Engineering*, vol. 7, no. 5, pp. 115–126, 1983.

[14] R. Balaka and A. Rachman, "Pitch angle effect for horizontal axis river current turbine," *Procedia Enginneering*, vol. 50, pp. 343–353, 2012.

[15] T. A. De Jesus Henriques, H. T. S., I. Owen, and P. R. J., "The influence of blade pitch angle on the performance of a model horizontal axis tidal stream turbine operating under wave current interaction," *Energy*, vol. 102, no. 1, pp. 166–175, 2016.

[16] J. N. Goundar, M. R. Ahmed, and Y. H. Lee, "Numerical and experimental studies on hydrofoils for marine current turbines," *Renewable Energy*, vol. 42, pp. 173–179, 2012.

[17] M. Anyi and B. Kirke, "Hydrokinetic turbine blades: Design and local construction techniques for remote communities," *Energy for Sustainable Development*, vol. 15, no. 3, pp. 223–230, 2011.

[18] D. Kumar and S. Sarkar, "A review on the technology, performance, design optimization, reliability, techno-economics and environmental impacts of hydrokinetic energy conversion systems," *Renewable and Sustainable Energy Reviews*, vol. 58, no. Supplement C, pp. 796 – 813, 2016.

[19] N. D. Laws and B. P. Epps, "Hydrokinetic energy conversion: Technology, research, and outlook," *Renewable and Sustainable Energy Reviews*, vol. 57, no. Supplement C, pp. 1245 – 1259, 2016.

[20] M. R. Ahmed, "Blade sections for wind turbine and tidal current turbine applications-current status and future challenges," *International Journal on Energy Research*, vol. 37, no. 7, pp. 829–844, 2012.

[21] E. Chica, F. Pérez, A. Rubio-Clemente, and A. S., "Design of a hydrokinetic turbine," *WIT Transactions on Ecology and The Environment. Wessex Institute of Technology*, vol. 195, pp. 137–148, 2015.

[22] E. Chica, F. Pérez, and A. Rubio-Clemente, "Rotor structural design of a hydrokinetic turbine," *International Journal of Applied Engineering Research*, vol. 11, no. 4, pp. 2890–2897, 2016.

[23] N. Kolekar and A. Banerjee, "A coupled hydro-structural design optimization for hydrokinetic turbines," *Journal Renewable Sustainable Energy*, vol. 5, no. 053146, pp. 1–22, 2013.

[24] G. Zhao, R.-S. Yang, Y. Liu, and P.-F. Zhao, "Hydrodynamic performance of a vertical-axis tidal-current turbine with different preset angles of attack," *Journal of Hydrodynamics, Ser. B*, vol. 25, no. 2, pp. 280–287, 2013.

[25] S. S. Mukherji, N. Kolekar, A. Banerjee, and R. Mishra, "Numerical investigation and evaluation of optimum hydrodynamic performance of a horizontal axis hydrokinetic turbine," *Journal of Renewable and Sustainable Energy*, vol. 3, no. 063105, pp. 1–18, 2011.

[26] R. C. Adhikari, J. Vaz, and D. Wood, "Cavitation inception in crossflow hydro turbines," *Energies*, vol. 9, no. 237, pp. 1–12, 2016.

[27] A. Muratoglu and M. I. Yuce, "Design of a river hydrokinetic turbine using optimization and cfd simulations," *Journal of Energy Engineering*, vol. 143, no. 4, p. 04017009, 2017.

[28] G. Tampier, C. Troncoso, and F. Zilic, "Numerical analysis of a diffuser-augmented hydrokinetic turbine," *Ocean Engineering*, vol. 145, pp. 138–147, 2017.

[29] P. Silva, T. Oliveira, A. Brasil, and J. Vaz, "Numerical study of wake characteristics in a horizontal-axis hydrokinetic turbine," *Anais da Academia Brasileira de Ciências*, vol. 88, no. 4, pp. 2441–2456, 2016.

[30] Y. Ren, B. Liu, T. Zhang, and Q. Fang, "Design and hydrodynamic analysis of horizontal axis tidal stream turbines with winglets," *Ocean Engineering*, vol. 144, no. Supplement C, pp. 374 – 383, 2017.

[31] D. P. Coiro, U. Maisto, F. Scherillo, S. Melone, and F. Grasso, "Horizontal axis tidal current turbine: numerical and experimental investigations," in *Proceeding of Offshore Wind and Other Marine Renewable Energies in Mediterranean and European Seas, European Seminar, Rome, Italy*. Citeseer, 2006, pp. 20–22.